

This is a postprint/accepted version of the following published document:

Riol Martín, J.; Pérez Leal, R.; García Armada, A. Design of DMRS schemes for 5G vehicular communications. In: *2021 IEEE 93rd Vehicular Technology Conference (VTC2021-Spring), 25-28 April 2021, Helsinki, Finland (Virtual edition)*. IEEE, 2021, 5 pp.

DOI: <https://doi.org/10.1109/VTC2021-Spring51267.2021.9449011>

© 2021 IEEE. Personal use of this material is permitted. Permission from IEEE must be obtained for all other uses, in any current or future media, including reprinting/republishing this material for advertising or promotional purposes, creating new collective works, for resale or redistribution to servers or lists, or reuse of any copyrighted component of this work in other works.

Design of DMRS schemes for 5G vehicular communications

Juan Riol Martín⁽¹⁾, Raquel Pérez Leal⁽¹⁾, Ana García Armada⁽¹⁾

juanriol@msn.com, rpleal@ing.uc3m.es, agarcia@tsc.uc3m.es

⁽¹⁾ Dept. of Signal Theory and Communications Universidad Carlos III de Madrid.

Abstract- The arrival of the fifth generation (5G) of mobile communications is boosting vehicular communications, an important use case addressed in the recent years. LTE introduced a sidelink radio interface through which user equipment would communicate directly with no necessary dependence on the network, named PC5. 5G has defined its own sidelink interface, NR-Sidelink, envisaged to improve PC5. This paper analyses the use of Demodulation Reference Signals (DMRS) to estimate the channel in sidelink communications. Improving several mappings proposed by the standards, the main contribution proposed in this paper is a new DMRS mapping with a better performance. The proposed Unequal Pilot Spacing (UPS) mapping can enhance the standard with a satisfactory trade-off between performance and overhead.

Index terms- 5G, DMRS, PC5, sidelink interface, vehicular communications

I. INTRODUCTION

The arrival of 5G is foreseen to be a turning point not only for the telecommunications industry, but also for many other verticals like the automotive sector in which reliability and latency are particularly important to guarantee road security. Vehicle to Everything communications (V2X), which this article addresses, englobes a wide range of applications [1], [2]: intelligent roads, remote driving, platooning, etc. Two main candidate technologies address V2X: 802.11p and Cellular V2X (C-V2X), the first of which is based on the IEEE 802.11 protocol stack, while the second belongs to the 3GPP LTE family of standards. Both technologies are the adaptation of their corresponding protocols to fast-changing vehicular environments in which reliability and latency are critical whilst throughput is placed on hold, [3], [4]. In LTE/5G User Equipment's (UE) transmit and receive traffic communicating with the eNB through the Uu interface. C-V2X introduced in 2016 a new interface through which UEs could communicate with no eNB necessarily implied, under the name of PC5. Some upgrades on this interface were introduced in Release 15 (frozen in 2019), [5] with the definition of NR-Sidelink.

In such scenarios, the importance of DMRS to estimate the channel accurately is crucial. This work analyses the performance of different 5G DMRS configurations for sidelink V2X communications, defined in the standards [6]. A new DMRS mapping is proposed, so-called Unequal Pilot Spacing (UPS), that improves the performance of the standard mappings without increasing the overhead. Both the standard and new proposed mappings are evaluated and compared in terms of symbol error rate (SER) for QPSK and 16-QAM constellations.

Previous works have addressed this topic for OFDM systems. Reference [7] proposes adaptive pilot-symbol patterns that follow changing channel statistics to maximize throughput and [8] considers a power allocation mechanism between pilot symbols and data to maximize the sum symbol rate. However, neither consider the NR-Sidelink frame structure, whilst this paper focuses on NR C-V2X use case. Besides, UPS aims to minimize SER, not maximize throughput, and only considers pilot distribution and not power allocation.

The rest of the paper is organized as follows: section II introduces Sidelink Communications and their requirements and benefits. Section III introduces the system model and section IV the proposed mapping. Then, section V states and analyses the numerical results, and section VI finishes with some general conclusions.

II. SIDELINK COMMUNICATIONS

Sidelink communications and the interface PC5 have been developed since Release 14. PC5 has two operational modes, named in the standard as Mode 3 and Mode 4, both displayed in Figure 1. The main difference between these two modes is the resource allocation methodology, which is centralized for Mode 3 and distributed for Mode 4. In this sense, the physical resource blocks (PRBs) that each UE uses to transmit information are assigned by the eNB in Mode 3, whilst in Mode 4 other distributed mechanisms are used. Furthermore, Mode 3 relies on the eNB for signalling and scheduling operations so UEs' coverage must be assured for this mode.

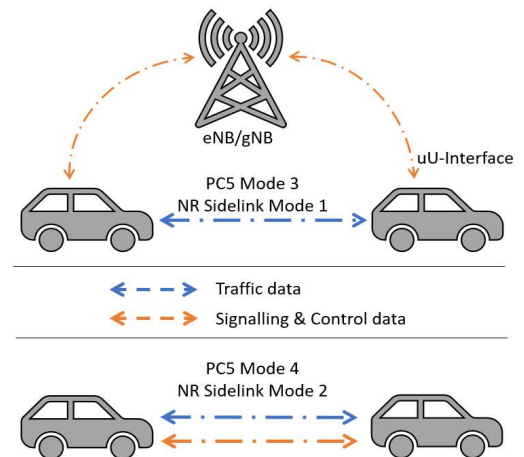


Fig. 1. C-V2X operation modes for PC5. Up: in-coverage mode. Down: out-of-coverage mode.

Although several benefits derive from the definition of PC5 (mitigation of the Doppler Effect, palliation of the latency problem since information is delivered directly between UEs), nevertheless, it entails a series of disadvantages to deal with, such as resource scheduling or synchronization. To remediate these disadvantages, Release 15 and 16, [9], along with other academic papers have studied and proposed several mechanisms to be applied in 5G, in which PC5 has its homonymous interface, the NR sidelink. NR sidelink has two operational modes, Mode 1 and Mode 2 which are equivalent to PC5's Mode 3 and Mode 4 respectively. There are some differences between PC5 and NR sidelink, however both sidelink interfaces use the 5.9 GHz band. This band is licensed to Intelligent Transportation Systems (ITS) from 5.85 to 5.925 GHz in which 802.11p and C-V2X must co-exist. Another important aspect is the Modulation and Coding Scheme (MCS). 5G aims to gain flexibility to address different use cases thanks to the different MCS and subcarrier spacing schemes. Table I, reconstructed from [10], summarizes these and other relevant features of these two sidelink interfaces.

As seen in Table I, another noticeable difference is the multiplexing in both generations, time-multiplexed in NR and frequency-multiplexed in PC5. In NR sidelink, the DMRS are placed in the same time instant for all the subcarriers, occupying each the duration of an OFDM symbol. In 5G the relation between the duration of a slot composed by 14 symbols and a subframe of 1 ms depends on the numerology. Hence, the scheduling in NR will be done per slot while in PC5 it is done per subframe. Whilst in PC5 there are 4 DMRS symbols in fixed positions per subframe, in NR sidelink there are flexible front-loaded schemes of DMRS scheduled for a full slot of 14 symbols with one to four DMRS per slot, [11].

TABLE I
COMPARISON BETWEEN PC5 AND NR SIDELINK

	PC5	NR Sidelink
<i>Standardized</i>	Release 14	Release 15
<i>MCS</i>	QPSK, 16-QAM	QPSK, 16/64-QAM
<i>Waveform</i>	SC-FDMA	OFDM
<i>Retransmissions</i>	Blind	HARQ
<i>Control & data multiplex</i>	FDM	TDM
<i>DMRS</i>	4/subframe	Flexible
<i>Sub-carrier spacing</i>	15 KHz	15/30/60/120 KHz
<i>Scheduling</i>	1 subframe	(multi-mini) slot
<i>Sidelink modes</i>	Modes 3 & 4	Modes 1 & 2
<i>Channel bandwidth</i>	10 MHz	10 MHz

NR sidelink communications are mapped in uplink channels. Thus, sidelink communication structure is defined in the same Technical Study as the NR uplink channel. Particularly, the DMRS structure of the uplink channel is defined in TS 38.211 in its section 6.4.1.1, [6]. In its version 15.2.0, already standardized by ETSI, DMRS structures depend on three parameters: the configuration type (either 1 or 2), the frequency hopping (enabled or disabled) and the mapping type (either A or B, [6]). There are other parameters belonging to higher layers that condition the DMRS scheme, both of which may be seen in Table 6.4.1.1 from [6] for the case of no frequency hopping. Every scheme contains an l_0 parameter which is the position of the first DMRS symbol. The difference between A and B mappings is the calculation of l_0 and the parameter *dmrs-AdditionalPosition*. Regardless of the

second parameter, l_0 is given by a higher-layer parameter for mapping type A and equals 0 for mapping type B. Table II displays the 14-symbol slot DMRS schemes for both mapping types and the 4 *dmrs-AdditionalPosition* values.

TABLE II
NR PUSCH DMRS POSITIONS (NO FREQUENCY HOPPING), [6]

	0	1	2	3
<i>Mapping A</i>	l_0	$l_0, 11$	$l_0, 7, 11$	$l_0, 5, 8, 11$
<i>Mapping B</i>	l_0	$l_0, 10$	$l_0, 5, 10$	$l_0, 3, 6, 9$

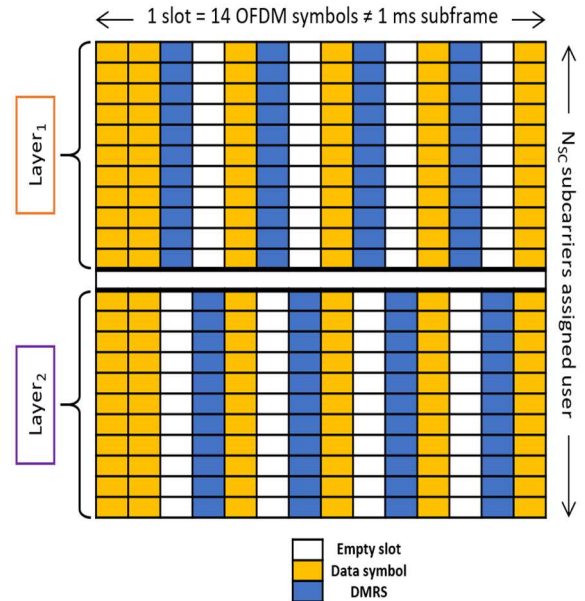


Fig. 2. NR two-layer orthogonal DMRS MIMO scheme.

A slot of 14 OFDM symbols may include from 1 to 4 DMRS, depending on the Channel Quality Indicator (CQI). The lower the noise and the channel variability, the less DMRSs are needed to estimate the channel correctly. This table applies not only for Single Input Single Output (SISO) schemes, but also for Multiple Input Multiple Output (MIMO) schemes. As for the DMRS mapping in MIMO schemes, DMRSs must be orthogonal for each MIMO layer of a user. To that end, in the resource element in which a DMRS is sent for a certain layer, no information must be sent in the rest of the layers. Figure 2 displays the outlook of a MIMO scheme with two layers.

III. SYSTEM MODEL

This section introduces the system model of the NR sidelink and it explains the assumptions and simplifications made to facilitate the problem, which do not undermine the results' validity. Figure 3 represents the system model, in which the waveform is Cyclic Prefix OFDM and the channel model is Clustered Delay Line (CDL) as a faithful representation of a 5G channel, [12], detailed in section V. As in the standard, [11], information is transmitted in the PUSCH channel. Synchronization between the transmitter and the receiver is assumed. The channel effect is estimated for DMRS symbols and extended to the rest of symbols by a linear interpolation in the time domain. Hence, the output is a time-frequency grid with the channel response for each OFDM symbol.

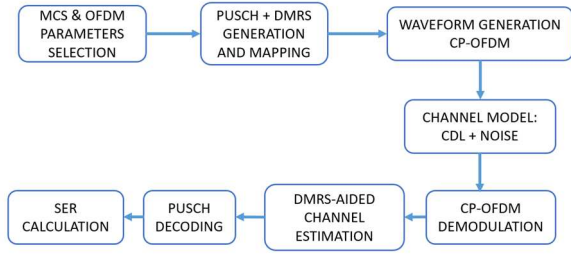


Fig. 3. System model block diagram.

Regarding the DMRS schemes, 3 different mappings have been evaluated and compared. The first 2 are Mapping A and Mapping B, both belonging to the standard. However, a third one has been tested. This proposed mapping is the main contribution of the paper and is explained in next section. As for MIMO, for the system model we assume the same number of transmitting and receiving antennas and thus an MxM system. Such system may be modelled through MxM different subchannels h_{ij} where i and j sub-indexes refer to the receiving and transmitting antenna respectively. Therefore, for a time instant n , and subcarrier k the system may be modelled with the following equations, where Tx are the transmitted symbols and Rx are the received ones. Note that in each time instant, MxM different subchannels are estimated.

$$\begin{bmatrix} Rx_1^{n,k} \\ Rx_2^{n,k} \\ \vdots \\ Rx_M^{n,k} \end{bmatrix} = \begin{bmatrix} h_{1,1}^{n,k} & h_{1,2}^{n,k} & \dots & h_{1,M}^{n,k} \\ h_{2,1}^{n,k} & h_{2,2}^{n,k} & \dots & h_{2,M}^{n,k} \\ \vdots & \vdots & \ddots & \vdots \\ h_{M,1}^{n,k} & h_{M,2}^{n,k} & \dots & h_{M,M}^{n,k} \end{bmatrix} \times \begin{bmatrix} Tx_1^{n,k} \\ Tx_2^{n,k} \\ \vdots \\ Tx_M^{n,k} \end{bmatrix}$$

IV. UPS MAPPING

This section explains the proposed mapping that enhances the standard's ones. It is denoted as Unequal Pilot Spacing (UPS) mapping. In the standard, [6], the positions of DMRS are fixed for every slot depending on the chosen mapping. This paper proposes a different scheme such that for a mapping with n DMRS, slots are transmitted alternatively with $n+1$ and $n-1$ DMRS. In average, the same number of symbols are mapped to DMRS and to data, yet performance in terms of SER is improved. Table III details the position of each DMRS.

TABLE III
DMRS POSITIONS FOR THE PROPOSED UPS MAPPING

Number of DMRS	1	2	3	4
DMRS positions	4	4,12	2,6,9,13 4,12	2,5,8,11,14 4,8,12

The UPS is applied just for schemes with 3 and 4 DMRS. The rationale behind this method relies in the fact that the performance improvement between 5 and 4 DMRS is higher than the degradation between 4 and 3 DMRS respectively, whilst in average, the same number of DMRS are sent. In each slot, the pilot symbols are as evenly spaced as possible. However, this logic does not apply for 1 and 2 DMRS schemes; for those cases, fixed positions for the DMRS are used, like the standard does. For these two cases, different DMRS positions have been tested, and the schemes with the best performance have been chosen. As for MIMO for UPS mapping, two possible configurations were used to adapt the UPS mapping to a MxM MIMO system with pilot orthogonality. Both schemes may be found in Table IV particularized for a 2x2 scheme, named as parallel UPS (up) and cross UPS (down).

TABLE IV
DMRS POSITIONS MIMO UPS: PARALLEL & CROSS

		Even slots	Odd slots
Parallel UPS	Layer ₁	2,5,8,11,14	4,8,12
	Layer ₂	1,4,7,10,13	3,7,11
Cross UPS	Layer ₁	2,5,8,11,14	4,9,12
	Layer ₂	4,9,12	2,5,8,11,14

Comparing Table III with Table IV, the adaptation to MIMO entails some modifications in the schemes to keep pilot orthogonality. For the parallel UPS both layers would have the same number of DMRS in the same slots, so all the pilots of one of the layers must be displaced one symbol. On the other hand, for cross UPS, in a certain slot the two layers would have $n-1$ and $n+1$ DMRS respectively. Hence, according to the scheme displayed in Table III, both layers would have a DMRS in symbol 8. Thus, the pilot placed in symbol 8 in the layer with 3 DMRS in that timeslot is displaced to symbol 9 to maintain orthogonality.

V. NUMERICAL RESULTS

This section analyses the effect of the different DMRS schemes in terms of SER. There are other parameters whose effect in the SER is analysed in this section, such as the channel variability and the used constellation. CDL-E channel subtype has been used since it represents a Line of Sight (LoS) environment corresponding to a Mode 1 sidelink scenario. As for the delay spread, its default value is 30 ns and if different, the value will be specified onwards. The MIMO scheme is set as a 2 transmitting and 2 receiving antennas (2X2). The rest of the parameters regarding the channel are left as default, [13]. The actual default values that have been used for the simulations are displayed in Table V.

TABLE V
SIMULATION INVARIANT PARAMETERS

Parameter	Value
Channel bandwidth	10 MHz
Useful Subcarriers	600
Total Subcarriers	1024
Cyclic Prefix length	80 samples
Multiplexing freq. offset	212 subcarriers
Transmitted 14-symbol slots	100,000
CDL channel frequency	5.9 GHz
Channel speed	20, 120, 240 km/h
Constellation	QPSK/16-QAM
MIMO scheme	2x2

A. Mapping comparison and effect of channel variability

This first subsection compares the performance in terms of SER of the different mappings and channel variabilities. For each DMRS scheme of both mapping types, only results with 16-QAM are shown. For mapping type B $l_0=0$, while for mapping type A, $l_0=2$ or 3 depending on the parameter *dmrs-TypeA-Position* (see Table II), [6]. Mapping A is set such that $l_0=3$, since this value was found to provide a better performance in terms of SER compared to mapping B and mapping A with $l_0=2$. Only the curves for the mappings with 3 and 4 DMRS are plotted, since those are the most relevant ones due to the configuration of the UPS mapping. In fact, behaviour for 1 and 2 DMRS schemes is seamless for all the mappings, so there is no need to plot them.

Two different channel speeds are tested to analyse the effect of the variability of the channel on the performance in terms of SER. The channel speed is defined as the relative speed between the two involved UEs. Two different situations will be tested depending on whether the UEs go in the same or opposite direction, these are:

a) UEs in same direction (A): it shall be quite usual for many applications like platooning or sensor sharing between vehicles. If the involved UEs are following the same direction (in the same highway lane or street), channel variability will be low regardless of the environmental situation. The selected value of the relative vehicle speed to account for the channel variability in this situation is 20 km/h.

b) UEs in opposite direction (B): communication between vehicles in opposite directions in a highway has a clear objective: avoid accidents and fatalities. Not only a direct crash between the involved UEs, but also a notification of hazard, bad weather or roadworks that may have been unnoticed. Assuming the maximum speed allowed in highways is 120 km/h and with vehicles driving in opposite directions, the relative speed is taken as 240 km/h.

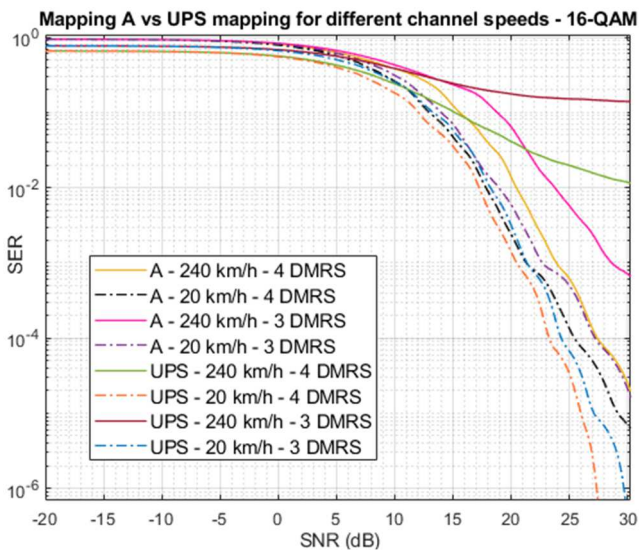


Fig. 4. Mappings' performance for different channel speeds

The UPS mapping has proved to be a better solution than any mapping in the standard for 3 and 4 DMRS schemes, due to the performance improvement with 5 and 4 DMRS over the degradation with 3 and 2 DMRS respectively. Furthermore, its robustness is more noticeable for worse SNR conditions. In fact, while the standard's mappings depart from the same value regardless of the number of DMRS, the proposed mapping achieves a better error ceil for 3 and 4 pilot schemes regardless of the channel speed, as well as a better error floor for the channel speed of 20 km/h.

The influence of the channel variability is greater for higher SNR, conditioning the error floor of the system. Dashed lines represent the channel speed of 20 km/h whilst solid lines represent the channel speed of 240 km/h. In this sense, for 20 km/h, UPS outperforms Mapping A. However, for 240 km/h it may be seen that UPS mapping performs better for worse SNR values, but Mapping A curves decrease more steadily from 10 dB onwards. For this channel speed, the SER error floor remains between 10^{-1} and 10^{-2} , whilst for 20 km/h, it falls to 10^{-6} . Hence, it may also be concluded that channel speed has a great influence in the system, especially for UPS mapping.

B. SISO vs MIMO

This subsection compares SISO and MIMO schemes with the parameters shown in Table V. In this case, the figures display results with QPSK constellation for Mapping A. To make it clearer, only schemes with 2 and 4 DMRS are plotted.

Figure 5 displays several crossing points between the MIMO and SISO schemes around 0 dB. The difference between schemes with 2 and 4 DMRS is smaller due to the lower-order constellation, yet it is higher in terms of SER for the MIMO scheme. The MIMO schemes depart from a lower error ceil but have an error floor between 10^{-1} and 10^{-2} . It may be concluded that the chosen MIMO scheme performs better for worse SNR values, and so SISO schemes are more effective at higher SNR values (from 0.3 dB onwards approximately).

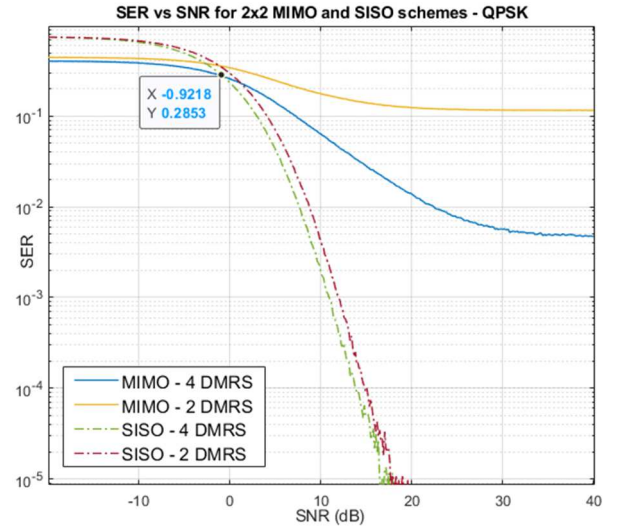


Fig. 5. SISO vs 2x2 MIMO SER comparison.

Next, we analyse the effect of the channel variability for MIMO schemes compared to SISO schemes. As concluded in previous subsection, the effect of the channel speed is more noticeable at higher SNR. Thus, only the most robust schemes with 4 DMRS will be plotted. As seen in Figure 6, for lower SNR values MIMO schemes perform better, yet their error floor is higher. While SISO schemes reach an error floor of around 10^{-5} , the MIMO schemes have a high error floor, especially for 240 km/h where the error floor stays at 0.3.

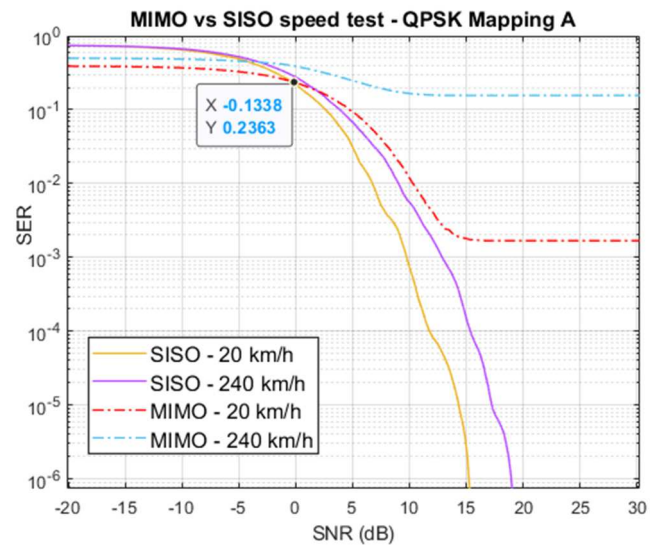


Fig. 6. Channel speed effect on the SER for 2x2 MIMO

Last, UPS mapping options (cross and parallel, as introduced in Section I) are compared with the standard mappings for a 2x2 MIMO scheme, shown in Figure 7. Only 4 DMRS schemes are plotted for both mappings. The UPS parallel mapping outperforms Mapping A and reaches a lower error floor, whilst the UPS cross mapping performs worse. UPS parallel mapping performs better than the UPS cross mapping because it maintains the intra-pilot distance, while UPS cross mapping modifies it to maintain pilot orthogonality.

As seen through the different subsections there is a trade-off between the amount of DMRS used and the SER, improved by the proposed UPS mapping, both for SISO and MIMO, following the same trend shown in the literature [14], [15].

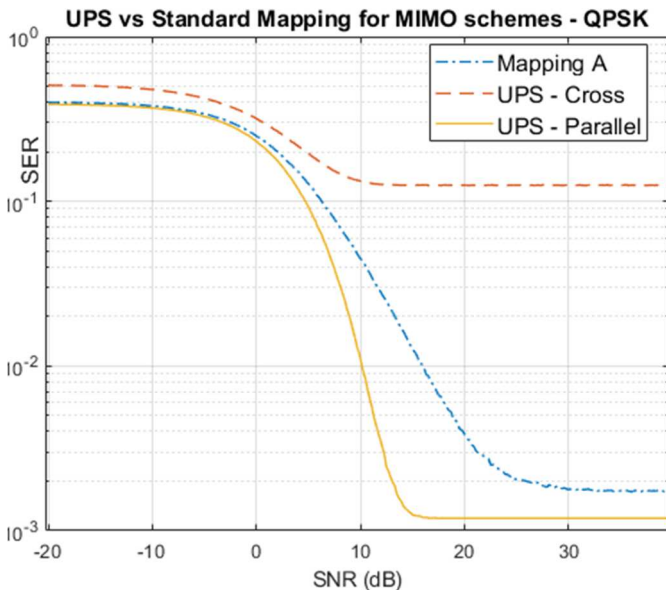


Fig.7. MIMO mappings comparison

VI. CONCLUSIONS

This paper has analysed the effect of different factors in C-V2X sidelink SISO and MIMO communications, such as the amount and distribution of DMRS and the variability of the channel. Besides, an alternative DMRS mapping that enhances the system performance in terms of SER is proposed, denoted as UPS mapping. It has been demonstrated that channel speed influences the system more than the number of DMR does. It has also been shown that MIMO schemes have a lower SER for lower SNR values, whilst they reach a SER floor for higher SNR values. Nevertheless, they provide a higher throughput than SISO thanks to the spatial multiplexing. Regarding the proposed UPS mapping, it has been tested against the standard mapping, proving that it performs better than the standard mapping for SISO and MIMO schemes. However, in high-speed situations, UPS starts performing worse from 17 dB SNR onwards. In conclusion, proposed UPS proves to be a valid alternative to the mappings in the standard, improving SER in most cases without increasing the overhead.

V2X is a exigent use case for wireless communications, and the sidelink interface paradigm opens a wide field of investigation: not only from the link level addressed in this study, it comprises other issues such as resource scheduling or sensing algorithms and procedures, [16]. As for the stringent requirements, these issues must be solved with no possibility of malfunction nor failure.

This work has been supported by the Spanish National Project TERESA-ADA (TEC2017-90093-C3-2-R) (MINECO/AEI/FEDER, UE).

REFERENCES

- [1] Visiongain, «Automotive Vehicle to Everything (V2X) Communications Market 2016-2026,» 2016.
- [2] IHS, «Identification and quantification of key socio-economic data to support strategic planning for the introduction of 5G in Europe,» 2017.
- [3] Y.-L. Tseng, «LTE-Advanced enhancement for vehicular communication,» *IEEE Wireless Communications*, vol. 22, n° 6, pp. 4-7, 2015.
- [4] A. Bazzi, G. Cecchini, M. Menarini, B. M. Masini y A. Zanella, «Survey and Perspectives of Vehicular Wi-Fi versus Sidelink Cellular-V2X in the 5G Era,» *Future Internet*, vol. 11, n° 122, 2019.
- [5] 3GPP, «ETSI TS 124 385; V16.2.0 Release 16; V2X services Management Object (MO),» October 2020. [Online]. Available: https://www.etsi.org/deliver/etsi_ts/124300_124399/124385/16.02.00_60/ts_124385v160200p.pdf. [Last access: 7 February 2021].
- [6] 3GPP, «ETSI TS 1.38.211; Version 16.2.0 Release 16; 5G; NR; Physical channels and modulation,» July 2020. [Online]. Available: https://www.etsi.org/deliver/etsi_ts/138200_138299/138211/16.02.00_60/ts_138211v160200p.pdf. [Last access: 7 February 2021].
- [7] M. Simko, P. S. R. Diniz, Q. Wang y M. Rupp, «Adaptive Pilot-Symbol Patterns for MIMO OFDM Systems,» *IEEE Transactions on Wireless Communications*, vol. 12, n° 9, pp. 2083-2088, 2013.
- [8] Z. Sheng, H. D. Tuan, Y. Fang, H. H. M. Tam y Y. Sun, «Data rate maximization based power allocation for OFDM System in a High-Speed Train Environment,» de *IEEE Global Conference on Signal and Information Processing (GlobalSIP)*, 2015.
- [9] 3GPP, «TS 38.213: NR; Physical layer procedures for control,» [Online]. Available: <https://portal.3gpp.org/desktopmodules/Specifications/SpecificationDetails.aspx?specificationId=3215>. [Last access: 7 February 2021].
- [10] G. Naik, B. Choudhury y J.-M. Park, «IEEE 800.11bd & 5G NR V2X: Evolution of Radio Access Technologies for V2X Communications,» 2019.
- [11] ETSI, «ETSI TS 138 300 V16.4.0,» [Online]. Available: https://www.etsi.org/deliver/etsi_ts/138300_138399/138300/16.04.00_60/ts_138300v160400p.pdf. [Last access: 6 February 2021].
- [12] W. Viriyasitavat, M. Boban y T. Hsin-Mu, «Vehicular Communications: Survey and Challenges of Channel and Propagation Models,» *IEEE Vehicular Technology Magazine*, vol. 10, n° 2, pp. 55-66, 2015.
- [13] MathWorks, «nrCDLChannel,» [Online]. Available: <https://es.mathworks.com/help/5g/ref/nrcdlchannel-system-object.html#d117e33637>. [Last access: 2020 February 4].
- [14] D. Wang, R. R. Sattiraju, A. Weinand y H. D. Schotten, «System-Level Simulator of LTE Sidelink C-V2X Communication for 5G,» 10 April 2019. [Online]. Available: <https://arxiv.org/abs/1904.07962>. [Last access: 18 Februar 2020].
- [15] R. Molina-Masegosa y J. Gozalvez, «LTE-V for Sidelink 5G V2X Vehicular Communications: A New 5G Technology for Short-Range Vehicle-to-Everything Communications,» *IEEE Vehicular Technology Magazine*, vol. 12, n° 4, pp. 30-39, 2017.
- [16] 3GPP, «3GPP TSG RAN WG1 Meeting #94bis, Sidelink resource allocation mechanism for NR V2X,» 3GPP, Chengdu, 2018.